JACS
JOURNAL OF THE AMERICAN CHEMICAL SOCIETY

Communication

pubs.acs.org/JACS

Spin Crossover in Anionic Cobalt-Bridged Fullerene $(Bu_4N^+)\{Co(Ph_3P)\}_2(\mu_2\text{-}Cl^-)(\mu_2\text{-}\eta^2,\eta^2\text{-}C_{60})_2$ Dimers

Dmitri V. Konarev,*[,†] Salavat S. Khasanov,[‡] Alexander F. Shestakov,[†] Manabu Ishikawa,[∥,§] Akihiro Otsuka,[∥,§] Hideki Yamochi,[∥,§] Gunzi Saito,[¶,⊥] and Rimma N. Lyubovskaya[†]

[†]Institute of Problems of Chemical Physics RAS, Chernogolovka, Moscow Region 142432, Russia

[‡]Institute of Solid State Physics RAS, Chernogolovka, Moscow Region 142432, Russia

[§]Division of Chemistry, Graduate School of Science, Kyoto University, Sakyo-ku, Kyoto 606-8502, Japan

[∥]Research Center for Low Temperature and Materials Sciences, Kyoto University, Sakyo-ku, Kyoto 606-8501, Japan

[¶]Faculty of Agriculture, Meijo University, 1-501 Shiogamaguchi, Tempaku-ku, Nagoya 468-8502, Japan

[⊥]Toyota Physical and Chemical Research Institute, 41-1, Yokomichi, Nagakute, Aichi 480-1192, Japan

Supporting Information

ABSTRACT: A spin crossover phenomena is observed in an anionic $(Bu_4N^+)\{Co(Ph_3P)\}_2(\mu_2\text{-}Cl^-)(\mu_2\text{-}\eta^2,\eta^2\text{-}C_{60})_2\cdot 2C_6H_{14}$ (**1**) complex in which two cobalt atoms bridge two fullerene molecules to form a dimer. The dimer has a triplet ground state with two weakly coupling Co^0 atoms (S = 1/2). The spin transition realized above 150 K is accompanied by a cobalt-to-fullerene charge transfer that forms a quintet excited state with a high spin Co^I (S = 1) and $C_{60}^{\bullet-}$ (S = 1/2).

Fullerene C_{60} forms a variety of coordination complexes with transition metals including iridium, nickel, palladium, ruthenium, and other metals.[1] These complexes are formed at the coordination of metal atoms to the 6−6 bonds of C_{60}. In general, such compounds contain monomeric fullerene units with weak charge transfer (CT) from metal to fullerene.[1] Coordination units can be also arranged in the dimers[2] or even polymers[3] through one[2a] or two[2d,e] bridged metal atoms or clusters.[2b,c] Neutral C_{60} cages are bound by two cobalt atoms in a zero oxidation state in $\{Co^0(Ph_3P)(C_6H_5CN)\}_2(\mu_2\text{-}\eta^2,\eta^2\text{-}C_{60})_2$ (**2**)[2d] and $\{Co^0(dppe)\}_2(\mu_2\text{-}\eta^2\text{:}\eta^2\text{-}\eta^2\text{-}[(C_{60})_2]$ (**3**)[2e] (dppe: 1,2-bis(diphenylphosphino)ethane). A rather strong magnetic coupling of the Co^0 spins with an exchange interaction of −28.6 K is attained in **2**.[2d] Developing functional transition metal−fullerene complexes that can combine high-spin metal atoms together with paramagnetic fullerene radical anions is a promising task to provide the coexistence of magnetic and conducting properties. Only several transition metal C_{60} complexes with Cp*IrI, Cp*IrCl, or $Cp^*Mo(CO)_2$ (Cp* is pentamethylcyclopentadienyl) have an essential negative charge on C_{60}. However, no paramagnetic species in these complexes have been found due to the diamagnetism of metal−C_{60}^- coordination units.[4]

In this work, we obtained the first anionic metal-bridged $\{Co(Ph_3P)\}_2(\mu_2\text{-}Cl^-)(\mu_2\text{-}\eta^2,\eta^2\text{-}C_{60})_2$ dimer. The anionic state of the dimer was realized due to an additional μ_2-coordination of the chloride anion to two cobalt atoms. The core part of the dimer $\{Co(Ph_3P)\}_2(\mu_2\text{-}\eta^2,\eta^2\text{-}C_{60})_2$ has a neutral triplet ground state and closely lying ionic quintet excited state providing a reversible temperature-activated spin crossover phenomena above 150 K. This transition is accompanied by CT from cobalt to fullerene. This is the first time such a phenomena has been observed for transition metal−fullerene complexes.

The complex was obtained as crystals through the use of a reduction method. Two $(Bu_4N^+)(C_{60}^{\bullet-})$ and $(Bu_4N^+)\{V^{IV}OPc(3-)^{\bullet-}\}$ salts were generated in a solution that was then reacted with one equivalent of $Co^{II}(Ph_3P)_2Cl_2$. The $V^{IV}OPc(3-)^{\bullet-}$ radical anions reduced $Co^{II}(Ph_3P)_2Cl_2$ so as to form $Co^I(Ph_3P)_2Cl$ and neutral $V^{IV}OPc(2-)$ precipitates from the solution. The interaction of $(Bu_4N^+)(C_{60}^{\bullet-})$ with $Co^I(Ph_3P)_2Cl$ produced a green−brown solution from which large black crystals of $(Bu_4N^+)\{Co(Ph_3P)\}_2(\mu_2\text{-}Cl^-)(\mu_2\text{-}\eta^2,\eta^2\text{-}C_{60})_2\cdot 2C_6H_{14}$ (**1**) are precipitated by *n*-hexane. The composition of **1** was determined by X-ray diffraction studies on a single crystal.

The crystal structure of **1** was studied at 85 and 300 K (see Supporting Information). Two bridging cobalt atoms are bonded to two C_{60} molecules in a dimer of **1** by a η^2 type (Figure 1a). The coordination to the 6−6 C_{60} bonds showed a slightly asymmetric feature with one shorter (2.034−2.046(2) Å) and one longer (2.104−2.125(**2**) Å) Co−C(C_{60}) bonds. The 6−6 bonds involved in the coordination are elongated up to 1.457−1.461(3) Å, whereas the average length of the other 6−6 C_{60} bonds in this complex is 1.396(**3**) Å. An essential elongation is also observed for the 6−5 bond connected to the coordinated 6−6 bonds with a length of 1.515(3) Å (the average length of other 6−5 bonds is 1.454(3) Å). This elongation is attributed to the π-back-donation.[1c] Both cobalt atoms coordinate to two 6−6 bonds belonging to one C_{60} hexagon, which results in a short Co···Co distance of 3.323(4) Å. In addition, the triphenylphosphine and bridging chloride anion coordinate to each cobalt atom. The length of the Co−P bonds is 2.2827(7) Å, whereas the Co−Cl bonds have a length of 2.4251(6) Å, and the Co−Cl−Co angle is 86.50(3)° (Figure 1b). The addition of the chloride anion to the dimer provides its monoanionic state that is compensated by the Bu_4N^+ cation. Two C_{60} molecules approach close to one another in the dimer, with the center-to-center (ctc)

Received: September 20, 2016
Published: December 12, 2016

DOI: 10.1021/jacs.6b09890
J. Am. Chem. Soc. 2016, 138, 16592−16595

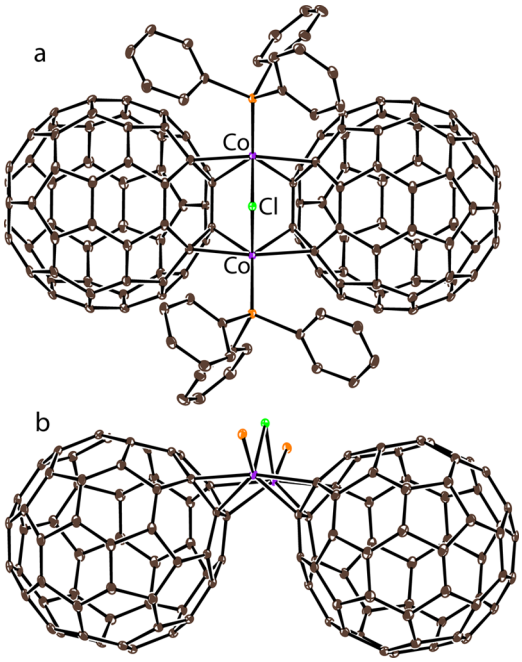

Figure 1. Molecular structure of $\{Co(Ph_3P)\}_2(\mu_2\text{-}Cl^-)(\mu_2\text{-}\eta^2,\eta^2\text{-}C_{60})_2$ viewed approximately along the direction perpendicular (a) and along (b) the line that passes through the two cobalt atoms. Carbon atoms are brown, phosphorus atoms are orange, cobalt atoms are violet, and chlorine atoms are green in this figure. Phenyl substituents of Ph_3P are not shown in panel b for the sake of clarity.

interfullerene distance being 9.692 Å. Similar or shorter ctc distances are observed also for dimers **2** and **3** bridge by two cobalt atoms (9.07−9.70 Å).[2d,e]

The magnetic properties of polycrystalline **1** were studied using the SQUID and EPR techniques, and similar EPR behavior is also confirmed for X-ray tested single crystal. There are two temperature intervals with different magnetic behaviors at $T <$ 150 and $T >$ 150 K. The effective magnetic moment of 2.43−2.48 μ_B is nearly constant in the 10−150 K range (Figure 2a; the temperature dependence of $\chi_M T$ is shown in Figure S4). This value is close to the magnetic moment calculated for the system of two noninteracting $S = 1/2$ spins per dimer (calculated value is 2.45 μ_B). The EPR spectrum of **1** at $T <$ 150 K shows two well resolved signals. The main broad signal with $g_1 = 2.1400$ and a line width (ΔH) of 58.96 mT at 120 K was attributed to Co^0 ($S = 1/2$), but a minor narrow signal with $g_2 = 1.9945$ and $\Delta H = 1.93$ mT at 120 K was attributed to $C_{60}^{\bullet-}$. The broad and narrow signals are preserved down to 4 K, and they show nearly paramagnetic temperature behavior (the spectrum of **1** at 4.2 K is shown in Figure S5). As the integral intensity of the narrow signal is less than 1% from that of the broad signal, we can conclude that the $C_{60}^{\bullet-}$ radical anions are present in **1** as impurity below 150 K, and the magnetic moment is defined by spins localized on Co^0. Weiss temperature estimated in the 150−10 K range of +2 K (Figure S3) indicate a weak ferromagnetic character attributable to the Co^0 spins. The magnetic moment decreases slightly below 10 K, and this is most probably due to intermolecular exchange effects. This results in the broadening of the main EPR signal and shifts its g-factor to larger values (Figure S8a,b). It is surprising that there is a lack of a strong magnetic exchange between the two adjacent cobalt centers with an electron configuration d^9 in the dimer. According to the general concept developed by Kahn[5] about the nature of magnetic interactions in binuclear d^9 complexes, an antiferromagnetic exchange is only realized when the overlapping of orbitals with one unpaired electron is permitted by symmetry. In the opposite case, when these orbitals have different symmetries, their overlap is zero, and consequently, only a weak ferromagnetic exchange is realized.

Equivalent metal centers in **1** have a coordination polyhedron in the form of a distorted pentagonal pyramid, which is formed by four carbon atoms of two fullerene ligands, one P atom in the pentagonal base, and the Cl^- anion at the vertex. The Cl−Co−P angle is 101.9(6)°, and the mean Cl−Co−C angle is 94.3(5)°. The upper x^2-y^2 and xy d-orbitals are degenerated for the regular pentagonal pyramid. The splitting of these orbitals at the Co center is only 1 meV or 9 cm^{-1}, as follows from the calculations of the mononuclear unit obtained from the dimer **1** by removing one of the $CoPPh_3$ fragments at the fixed positions of other atoms. The x^2-y^2 orbitals are symmetric, but the xy orbitals are antisymmetric with respect to the plane passing through the Cl, Co, and P atoms. Therefore, in the case of the electron configuration x^2-y^2(Co1), xy(Co2) overlapping between the magnetic orbitals is zero and a weak ferromagnetic exchange is expected (as observed in **1**). The true triplet $|x^2-y^2(Co1)\alpha\ xy(Co2)\alpha\rangle + |xy(Co1)\alpha\ x^2-y^2(Co2)\alpha\rangle$ and singlet state $|x^2-y^2(Co1)\alpha\ xy(Co2)\beta\rangle + |xy(Co1)\beta\ x^2-y^2(Co2)\alpha\rangle - |x^2-y^2(Co1)\beta\ xy(Co2)\alpha\rangle - |xy(Co1)\beta\ x^2 - y^2(Co2)\alpha\rangle$ are composed from equivalent configurations with interchanged d-orbitals in the Co-centers. This leads to the stabilization of the system due to resonant interactions, whose value is governed by the Coulomb integral $\langle x^2\text{-}y^2(Co1)xy(Co1)|1/r_{12}|\ x^2 - y^2(Co2)\ xy(Co2)\rangle$ for both states. For the alternative states, $|x^2 - y^2(Co1)\ x^2 - y^2(Co2)\rangle$ and $xy(Co1)\ xy(Co2)\rangle$, symmetry permitted overlapping of the magnetic orbitals results in the usual

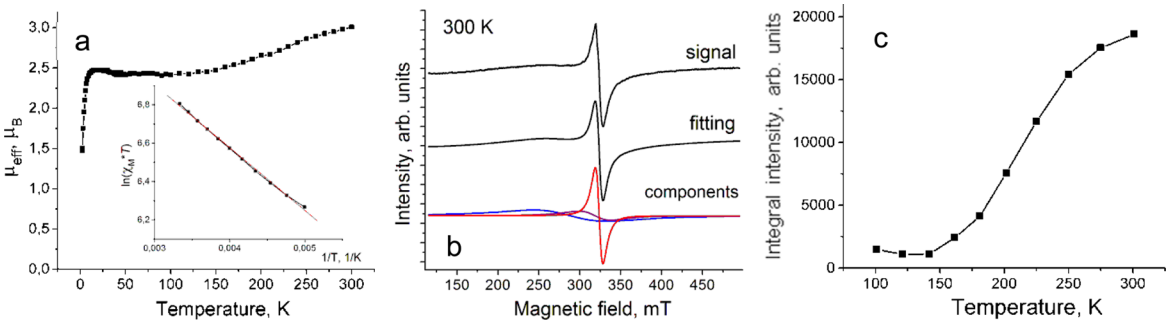

Figure 2. (a) Temperature dependence of the effective magnetic moment of **1** (determined by SQUID). (b) EPR signal of the polycrystalline **1** at 300 K and the fitting of the signal by three Lorentzian lines. (c) Integral intensity of the EPR signal of C_{60}. Inset for panel (a) shows the dependence of the natural logarithm of the molar magnetic susceptibility multiplied by T vs reverse temperature.

DOI: 10.1021/jacs.6b09890
J. Am. Chem. Soc. 2016, 138, 16592−16595

antiferromagnetic coupling being realized only due to the admixture of excited ionic states of the system,[6] which is the effect of the second order perturbation theory. This is the reason behind the weak ferromagnetic interactions in **1** rather than the antiferromagnetic interactions being due to a kinetic exchange.

A magnetic moment increase observed in **1** above 150 K (Figure 2a) is accompanied by the appearance of new EPR signals (Figure 2b), which allows for CT to be supposed from Co^0 ($S = 1/2$) to C_{60}^0 ($S = 0$) in order to form $C_{60}^{\bullet-}$ ($S = 1/2$) and high-spin Co^I ($S = 1$) (Figure 3). The magnetic moment

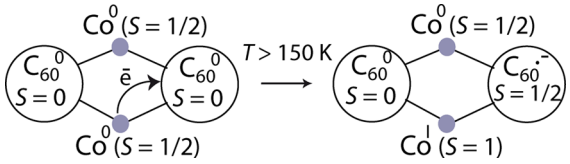

Figure 3. Schematic presentation of CT process realized in the $\{Co(Ph_3P)\}_2(\mu_2\text{-}Cl^-)(\mu_2\text{-}\eta^2,\eta^2\text{-}C_{60})_2$ dimer and resulted in a spin crossover phenomena above 150 K.

increases reversibly and monotonically above 150 K and reaches 3.03 μ_B at 300 K (Figure 2a). The magnetic moment increase allows us to suppose the formation of high-spin Co^I with $S = 1$ at the spin transition. In this case, a full transfer of one electron from Co^0 to C_{60} yields the quintet state of the dimer ($S = 1/2, 1/2, 1$) with a calculated magnetic moment of 3.75 μ_B. The value of 3.03 μ_B at 300 K corresponds to approximately 40% of the population of the quintet excited state.

Spin crossover essentially modifies the EPR spectrum of **1**. The signal at 300 K is well described by the superposition of three signals (Figure 2b). The relatively sharp signal (red line in Figure 2b) is assigned to be originated from $C_{60}^{\bullet-}$ due to the g-value and line width. The intensity increases abruptly above 150 K (Figure 2c), and this signal is well resolved on the background of broad signal from Co^0 (*vide infra*). The signal from $C_{60}^{\bullet-}$ is also noticeably broadened and shifts to larger g-factors with the temperature increase, as shown in Figure S6 ($g_2 = 1.9977$ and $\Delta H = 9.31$ mT at 300 K). Two broad signals (violet and blue lines in Figure 2b) are identified as those from Co. A broad signal of Co^0, which is a characteristic of the triplet ground state of the dimer, increases in intensity, broadens, and g-factor shifts to larger values as the temperature increases above 150 K ($g_1 = 2.2672$ and $\Delta H = 89.16$ mT at 300 K; Figure 2b, blue curve, Figure S8). Since the Co^I species with the $S = 1$ spin state can give a contribution to the EPR signal,[7] we suppose that the above-mentioned spectral changes are affected by this contribution. The shape of broad line cannot be well described by one Lorentzian line above 150 K because a new component appears. This component increases in intensity and broadens, and the g-factor shifts to larger values as the temperature increases (Figure S7). The origin of broad signal with $g_3 = 2.0364$ and $\Delta H = 39.90$ mT at 300 K (Figure 2b, violet curve) is most likely assigned to the Co^0 preserved in the quintet excited state. A smaller g-factor of this component in comparison to the broad signal of Co^0 described above is due to an additional contribution from $C_{60}^{\bullet-}$. Thus, the dimer in **1** shows reversible spin equilibrium behavior accompanied by the population of the quintet excited state with paramagnetic Co^I and $C_{60}^{\bullet-}$. A dependence of the natural logarithm of the molar magnetic susceptibility multiplied by T vs $1/T$ is linear in the 200−300 K range, thereby allowing the gap between the ground and excited states as 327 ± 5 K (Figure 2a, inset) to be determined. A similar estimation made from the EPR data yields close values.

According to the calculations, complex **1** has also a triplet ground state. Each Co atom has spin density of 1.07 in this state. A singlet state of the complex arises under the opposite orientation of the Co spins, and singlet state of the system with broken symmetry was not localized. The singlet state with closed shells has 11.8 kcal/mol higher energy than the triplet ground state. The quintet excited state is realized at parallel orientation of all spins under the transfer of one electron from Co^0 to C_{60}^0. It is higher in energy by 6.7 kcal/mol than the ground state that is several times greater than the energy gap estimated from the magnetic measurements. The reason is probably a lack of dynamic correlations in the DFT wave functions with equal spin density of both Co and C_{60}, which stabilizes the state with presumable localization of the hole and electron on one center by Coulomb interaction. A two-electron transfer with the formation of fully ionic symmetric structure with two $C_{60}^{\bullet-}$ and two Co^I atoms (the septet state) requires much more energy expenses, i.e., 28.8 kcal/mol, and cannot be realized in this system at the available temperatures. The structures of the quintet (one electron transfer) and septet (two electron transfer) states of **1** are shown in Figure 4. It is seen from

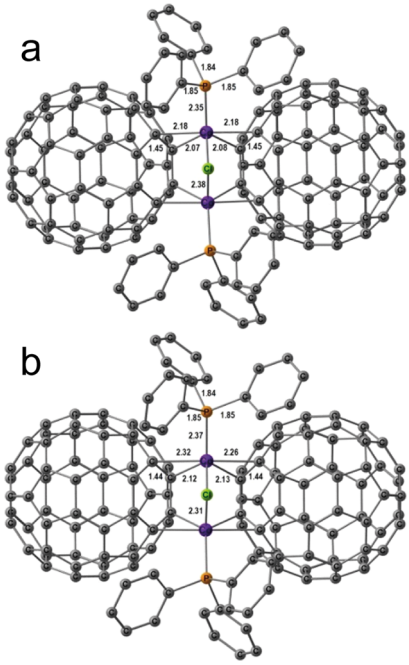

Figure 4. Calculated structures of complex in the ionic excited states with $S = 2$ for one electron transfer (a) and $S = 3$ for two electron transfer (b). The H atoms are omitted for clarity. Interatomic distances are given in Å.

calculations that electron transfer from cobalt to fullerene should shorten the Co−Cl bond and elongate of the Co−C(C_{60}) bonds. The structure at 300 K shows some changes in the bond lengths, but all of them are within the experimental error probably due to that the population of the excited ionic state at 300 K is only about 40%.

IR spectra of starting compounds and complex **1** are listed in Table S1 and Figure S1. The $F_{1u}(4)$ mode of C_{60} is sensitive to CT to the C_{60} molecule and is shifted from 1429 (neutral state) to 1390−1396 cm^{-1} in the radical anion state.[8] The absorption band of this mode is split into two bands observed at 1406 and 1418 cm^{-1}. The shift of these bands to the lower frequencies can

DOI: 10.1021/jacs.6b09890
J. Am. Chem. Soc. 2016, 138, 16592−16595

be explained by the π-back-donation[1c] (1418 cm^{-1}) as well the population of the excited ionic state of the dimer (1406 cm^{-1}).

The visible−NIR spectrum of **1** (Figure 5) is measured at 295 K. A broad and intense band is observed at 800 nm (1.55 eV),

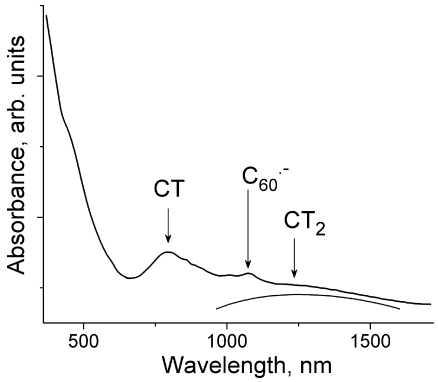

Figure 5. Spectrum of **1** in the visible and NIR range, measured in a KBr pellet that was prepared under anaerobic conditions. The charge transfer bands (CT, CT_2), and the band of $C_{60}^{\bullet-}$ are shown by the arrows.

whereas a weaker and wider band is observed at 1240 nm (1.00 eV0 (Figure 5). Both bands can be attributed to the spin allowed CT processes within the dimer i.e., to triplet−triplet transitions from the ground state. According to the theoretical calculations they most probably originate from the transfer of electron density from the metal atoms to the fullerene ligands. The absorption band at 1073 nm[8] unambiguously justified the presence of $C_{60}^{\bullet-}$ (Figure 5). It arises from electronic excitation of $C_{60}^{\bullet-}$ in thermally populated excited quintet state. The previously studied neutral cobalt-bridged dimer **2** also shows two CT bands in a solid state spectrum but at essentially higher energies (maxima at 630 and 920 nm (1.97 and 1.35 eV), respectively).[2d]

In conclusion, an anionic complex with cobalt-bridged fullerene dimers was obtained. The complex had a neutral triplet ground state with two Co^0 in a zero oxidation state (S = 1/2). The interaction between the Co^0 spins has a weak ferromagnetic character below 150 K because of weak overlapping of the magnetic orbitals in the dimers. The spin crossover to the quintet excited state is observed above 150 K and is accompanied by a cobalt-to-fullerene CT forming high-spin Co^I (S = 1) and $C_{60}^{\bullet-}$ (S = 1/2) species. This is the first example of a spin crossover phenomena occurring in fullerene coordination complexes. The spin transitions from low- to high-spin states are observed in metal (Fe^{II}, Fe^{III}, Co^{II}, Mn^{II}) complexes through the action of external stimuli, such as temperature, pressure, or light.[9] The CT, which causes spin state modulations, is known to take place between metal centers[10] and between metal and organic ligand.[11] Our report is the first example of a spin crossover phenomena occurring in fullerene coordination complexes. The spin transition in **1** could potentially be realized under light excitation on the wavelength of the metal-to-fullerene CT band. Fullerene transition metal complexes that can change their magnetic state under heat or light excitation are promising for organic spintronics and switchers. Such materials can be developed by applying proposed synthetic approach to changing fullerene units, bridged halide anions, or phosphine ligands at cobalt atoms. This work is now in progress.

■ ASSOCIATED CONTENT

Supporting Information

The Supporting Information is available free of charge on the ACS Publications website at DOI: 10.1021/jacs.6b09890.

IR spectra of starting compounds and **1**, EPR spectra of **1** in the 4−300 K range, synthesis, materials, and details of theoretical calculations (PDF)

X-ray crystal structure determination for **1** at 85 and 300 K (PDF) and (CIF)

■ AUTHOR INFORMATION

Corresponding Author

*konarev@icp.ac.ru

ORCID

Dmitri V. Konarev: 0000-0002-7326-8118

Notes

The authors declare no competing financial interest.

■ ACKNOWLEDGMENTS

The work was supported by Russian Science Foundation (project N 14-13-00028) and by JSPS KAKENHI (JP23225005 and JP26288035). Theoretical calculations were performed at Joint Supercomputer Center of Russian Academy of Sciences, Moscow, Russia.

■ REFERENCES

(1) (a) Balch, A. L.; Catalano, V. J.; Lee, J. W.; Olmstead, M. M.; Parkin, S. R. *J. Am. Chem. Soc.* **1991**, *113*, 8953−8955. (b) Bashilov, V. V.; Petrovskii, P. V.; Sokolov, V. I.; Lindeman, S. V.; Guzey, I. A.; Struchkov, Yu. T. *Organometallics* **1993**, *12*, 991−992. (c) Fagan, P. J.; Calabrese, J. C.; Malone, B. *Acc. Chem. Res.* **1992**, *25*, 134−142. (d) Balch, A. L.; Olmstead, M. M. *Chem. Rev.* **1998**, *98*, 2123−2165. (e) Lee, K.; Song, H.; Park, J. T. *Acc. Chem. Res.* **2003**, *36*, 78−86.

(2) (a) Jin, X.; Xie, X.; Tang, K. *Chem. Commun.* **2002**, 750−751. (b) Lee, K.; Song, H.; Kim, B.; Park, J. T.; Park, S.; Choi, M. G. *J. Am. Chem. Soc.* **2002**, *124*, 2872−2873. (c) Lee, G.; Cho, Y. J.; Park, B. K.; Lee, K.; Park, J. T. *J. Am. Chem. Soc.* **2003**, *125*, 13920−13921. (d) Konarev, D. V.; Troyanov, S. I.; Nakano, Y.; Ustimenko, K. A.; Otsuka, A.; Yamochi, H.; Saito, G.; Lyubovskaya, R. N. *Organometallics* **2013**, *32*, 4038−4041. (e) Konarev, D. V.; Troyanov, S. I.; Ustimenko, K. A.; Nakano, Y.; Shestakov, A. F.; Otsuka, A.; Yamochi, H.; Saito, G.; Lyubovskaya, R. N. *Inorg. Chem.* **2015**, *54*, 4597−4599.

(3) Konarev, D. V.; Khasanov, S. S.; Nakano, Y.; Otsuka, A.; Yamochi, H.; Saito, G.; Lyubovskaya, R. N. *Inorg. Chem.* **2014**, *53*, 11960−11965.

(4) (a) Konarev, D. V.; Troyanov, S. I.; Kuzmin, A. V.; Nakano, Y.; Khasanov, S. S.; Otsuka, A.; Yamochi, H.; Saito, G.; Lyubovskaya, R. N. *Organometallics* **2015**, *34*, 879−889. (b) Konarev, D. V.; Kuzmin, A. V.; Troyanov, S. I.; Khasanov, S. S.; Otsuka, A.; Yamochi, H.; Saito, G.; Lyubovskaya, R. N. *Dalton Trans.* **2015**, *44*, 9672−9681.

(5) Kahn, O. *Angew. Chem., Int. Ed. Engl.* **1985**, *24*, 834−850.

(6) Malrieu, J. P.; Caballol, R.; Calzado, C. J.; de Graaf, C.; Guihery, N. *Chem. Rev.* **2014**, *114*, 429−492.

(7) Krzystek, J.; Ozarowski, A.; Zvyagin, S. A.; Telser, J. *Inorg. Chem.* **2012**, *51*, 4954−4964.

(8) (a) Reed, C. A.; Bolskar, R. D. *Chem. Rev.* **2000**, *100*, 1075−1120. (b) Konarev, D. V.; Lyubovskaya, R. N. *Russ. Chem. Rev.* **2012**, *81*, 336−366.

(9) (a) Gaspar, A. B.; Ksenofontov, V.; Seredyuk, M.; Gütlich, P. *Coord. Chem. Rev.* **2005**, *249*, 2661−2676. (b) Gütlich, P.; Gaspar, A. B.; Garcia, Y. *Beilstein J. Org. Chem.* **2013**, *9*, 342−391.

(10) Kojima, N.; Aoki, W.; Itoi, M.; Ono, Y.; Seto, M.; Kobayashi, Y.; Maeda, Y. *Solid State Commun.* **2001**, *120*, 165−170.

(11) Tezgerevska, T.; Alley, K. G.; Boskovic, C. *Coord. Chem. Rev.* **2014**, *268*, 23−40.

DOI: 10.1021/jacs.6b09890
J. Am. Chem. Soc. 2016, 138, 16592−16595